

Surface diffusion of gold on quasihexagonal-reconstructed Au(100)

Artur Trembulowicz,^{1,*} Gert Ehrlich,¹ and Grazyna Antczak²

¹Materials Research Laboratory, University of Illinois at Urbana-Champaign, Urbana, Illinois, 61801, USA

²Institute of Experimental Physics, University of Wrocław, pl. M. Borna 9, 50-204 Wrocław, Poland

(Received 5 May 2011; revised manuscript received 10 December 2011; published 27 December 2011)

The scanning tunneling microscope has been used to measure the saturation island density N_x of gold on the hex-reconstructed Au(100) surface over a range of temperatures starting at 76 K. Assuming that the critical island size equals one, $\partial \ln N_x / \partial (1/T) = \chi E_d / k$, where χ is the scaling exponent, E_d gives the activation energy for surface diffusion, and k is the Boltzmann constant. The scaling exponent χ has been obtained as 0.26 ± 0.03 from measurements of the island density as a function of the deposition rate, indicating that diffusion is indeed one-dimensional (anisotropic) and the critical island size is unity. We therefore derive an activation energy of 0.32 ± 0.02 eV and a frequency prefactor of $2(\times 4^{\pm 1}) \times 10^{13} \text{ s}^{-1}$ for diffusion of gold on hex-reconstructed Au(100).

DOI: [10.1103/PhysRevB.84.245445](https://doi.org/10.1103/PhysRevB.84.245445)

PACS number(s): 68.35.B-, 68.37.Ef, 68.35.Fx

I. INTRODUCTION

With the increasing importance of miniaturization in everyday life, the significance of understanding basic processes occurring at surfaces grows. One of the important events controlling the stability of nanostructures is surface diffusion. We have investigated diffusion on gold, a widely used material in technology. To our surprise, the basic process—surface diffusion on real reconstructed surfaces of Au(100)—is not well understood. The long-range reconstruction of the gold surface^{1–10} establishes an environment not easy to investigate. The movement of gold atoms on the gold (100) plane is thus of scientific interest, but the kinetics of migration over this plane are still uncertain, and the complicated reconstruction is still a challenge to modeling.¹⁰

The only available diffusion measurements have been made by Günther *et al.*¹¹ with the scanning tunneling microscope (STM) to probe the saturation island density^{12,13} N_x at different temperatures T , given by nucleation theory as

$$N_x \sim \theta^{\chi/i} (D/F)^{-\chi} \exp(\chi E_i / ikT). \quad (1)$$

Here θ is the surface coverage, D gives the surface diffusivity, F is the rate of deposition, and E_i is the binding energy of the critical cluster i ; the binding energy is equal to zero for a critical cluster size of one. For two-dimensional diffusion $\chi = i/(i+2)$, whereas in one-dimensional (anisotropic) diffusion the exponent becomes $\chi = i/(2i+2)$.¹³

The first experiments on Au(100), carried out by Günther *et al.*,¹¹ found a scaling exponent $\chi = 0.37 \pm 0.03$, which initially appeared consistent with two-dimensional diffusion and a critical island size i of unity. Simulations, however, yielded values of the island density 7–10 times the experimentally determined density, and Günther *et al.*, therefore, assumed one-dimensional (anisotropic) diffusion and approximated the experimentally observed saturation density using $E_d \sim 0.2$ eV with a critical island size of three and a trimer binding energy of 0.6 eV.

These findings were challenged by Liu *et al.*,¹⁴ who considered the role of dimer diffusion, and with two-dimensional diffusion and a critical island size equal to one came up with an activation energy $E_d = 0.35$ eV for monomers and 0.45 eV for dimers, with a binding energy of 0.4 eV. Liu *et al.* assumed that reconstruction could not be so extensive that movement

changed from two- to one-dimensional, but they did not carry out control measurements and only reanalyzed the existing experimental data.

Subsequently the work of Günther *et al.*¹¹ was reanalyzed by Bartelt *et al.*¹⁵ who showed that the results of Günther *et al.*¹¹ must be preferred. However, the island densities of Günther *et al.* were measured at elevated temperatures, from 315 to 435 K, a fairly large range, over which dimers may be mobile. The extensive reconstruction of the Au(100) surface may indeed influence the dimensionality of diffusion, and we therefore decided to resolve existing uncertainties by carrying out measurements over a lower temperature range than explored previously.

II. RESULTS

In order to explore clusters with a critical nucleus of one, we have repeated studies of the saturation island density of gold on Au(100) at low temperatures and at a pressure $< 10^{-10}$ Torr. Measurements of the island density were done with an Omicron VT STM, always scanning at 100 K or lower, cooled with liquid helium to temperatures as low as 76 K; the temperature was measured by a thermocouple in contact with the top surface of a dummy sample. Values of the island density were determined separately a few times and were then averaged. An image of the clean gold surface, obtained by repeated ion bombardment at 1 keV for 15 min with argon, followed by 10 min annealing at 850 K, is shown in Fig. 1(a). The unit cell there, (6×30) , comes about as the outermost layer is reconstructed into an arrangement resembling a quasihexagonal structure on top of a square lattice, illustrated in Fig. 2. The surface depicted in Fig. 1(a) is very similar to that of Pt(100)¹⁶ and has channels half a unit cell long in the $[01\bar{1}]$ direction. This is also demonstrated in Figs. 1(b) and 1(c) by the STM profiles along A and B across a unit cell. Reconstructed domains are observed with channels along $[011]$ as well as $[01\bar{1}]$.

When gold atoms are evaporated onto the Au(100) surface at ~ 200 K from a heated source, either a tungsten basket or a graphite crucible, stringlike islands are formed along the $\langle 011 \rangle$ rows, as is apparent in Fig. 3(a). Many of the same structures are seen at 236 K, in Fig. 3(b), but at a temperature of 120 or 90 K, in Figs. 3(c) and 3(d), the islands

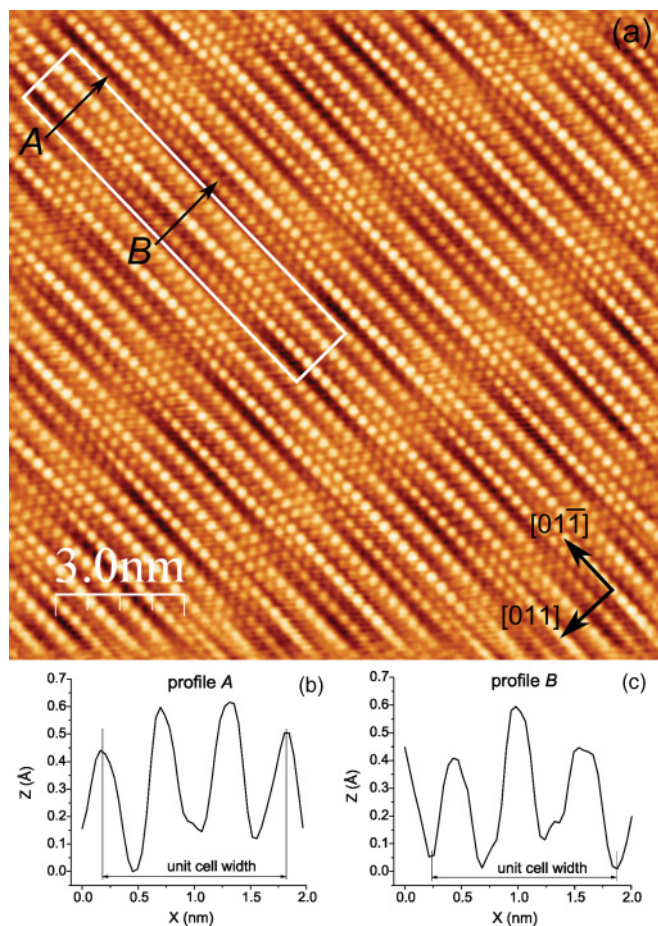


FIG. 1. (Color online) (a) STM image of reconstructed Au(100) surface at 3 nA and 2 mV, showing a (6×30) unit cell after bombardment at 1 keV with argon ions and annealing at 850 K. Scanning is along the horizontal. (b) Profile along A across a unit cell. (c) Profile along B.

are essentially round. Apparent in the shape of the islands is the slow diffusion rate with D/F below 10^5 , known as the postnucleation regime. At 200 K, the aspect ratios of the islands vary but are as large as 1:37, which suggests preferred unidirectional (anisotropic) diffusion. Deposition is continued until the island layer is saturated, and the density of islands is obtained, as illustrated in Fig. 4 at 100, 150, and 200 K. As the temperature is increased from 100 K, the saturation island density diminishes but is still on the horizontal part of the curve of island density versus coverage. Saturation in general was reached by depositing the same amount of gold at other temperatures. An interval of ~ 75 min was necessary to reach saturation; thereafter, up to one-half hour was spent for the change from deposition to scanning temperature. A few hours were devoted to measurements. We assume that all single atoms attached to existing islands during the deposition, and there is no significant postdeposition activity during cooling to 100 K.

The diffusivity D can be written as a function of the temperature as

$$D = D_0 \exp(-E_d/kT). \tag{2}$$

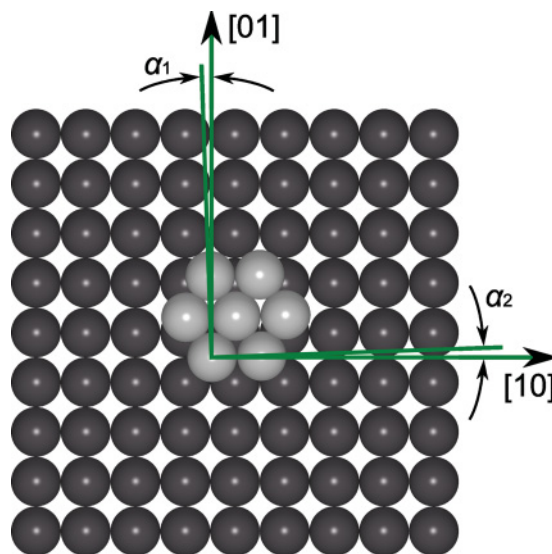


FIG. 2. (Color online) Model of quasi-hexagonal surface layer on Au(100) lattice (Ref. 6). $\alpha_1 = \alpha_2 \approx 0.7^\circ$ with respect to the [01] direction.

For the diffusivity expressed in terms of the jump length, the prefactor D_0 is given by the essentially constant frequency prefactor ν . As is clear from Eq. (1), measurement of the saturation island density N_x at different temperatures, but at constant deposition rate F and constant coverage, should yield the activation energy E_d for diffusion, inasmuch as

$$\partial \ln N_x / \partial (1/T) = -\chi \partial \ln D / \partial (1/T) = \chi E_d / k. \tag{3}$$

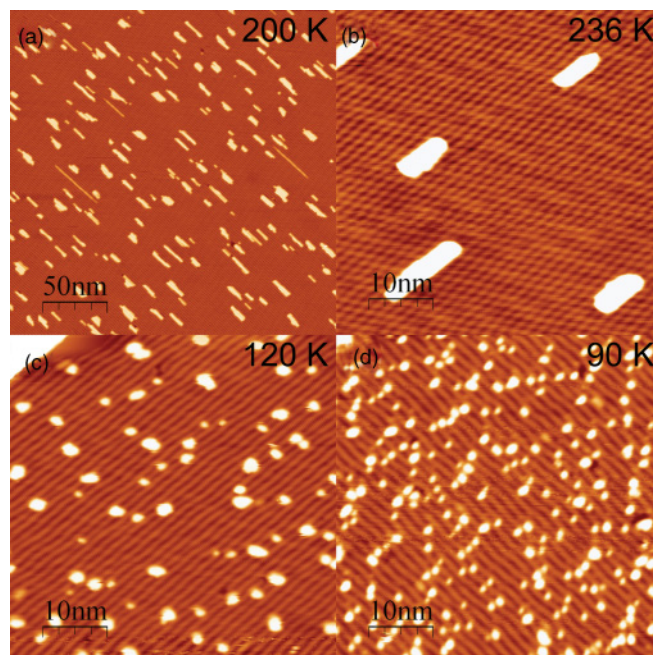


FIG. 3. (Color online) STM image of gold islands deposited on reconstructed Au(100). (a) For Au(100) temperature of 200 K, islands are stringlike. Scanning is at 100 K with 0.5 nA and 1 V. (b) At $T = 236$ K islands are stringlike. (c) At $T = 120$ K and (d) at $T = 90$ K, islands are round.

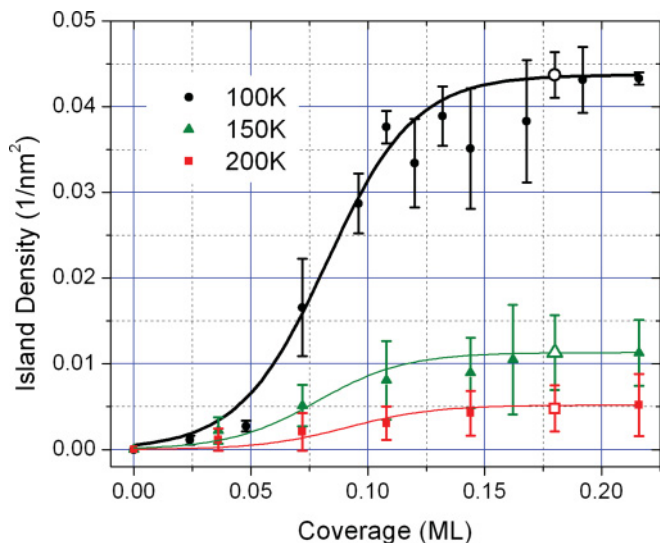


FIG. 4. (Color online) Plot of island density versus coverage of gold on reconstructed Au(100) at $T = 100, 150,$ and 200 K. Open symbols indicate saturation density.

This, of course, assumes that the critical island size is equal to one. A plot of the logarithm of the saturation island density N_x against the reciprocal temperature $1/T$ over the range from 76 to 234 K is given in Fig. 5, with the line drawn only as a guide. Scanning was always done at 100 K. On the assumption that the critical cluster size is unity and diffusion is highly anisotropic (one dimensional), the slope of the curve from 156 to 236 K yields an activation energy of 0.32 ± 0.02 eV.

The important question now is the size of the critical cluster: is it indeed unity? To explore this matter, we have in addition measured the island density N_x as a function of

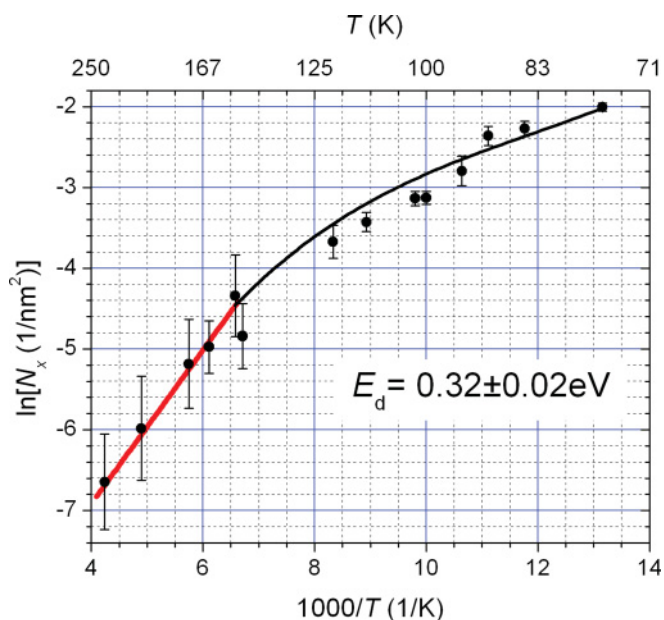


FIG. 5. (Color online) Plot of logarithm of the gold saturation island density on reconstructed Au(100) as a function of $1/T$. Analysis assumes one-dimensional (anisotropic) diffusion and a critical island size of one. E_d derived for data from 236 to 156 K, shown by heavy (red) line. Curve is for guidance only.

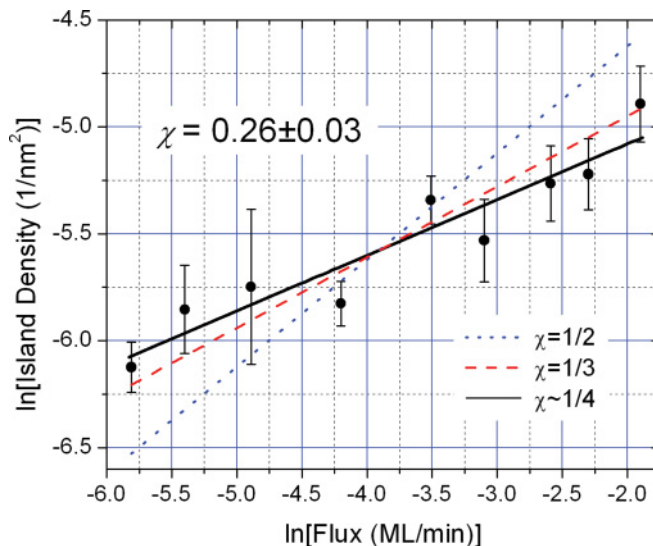


FIG. 6. (Color online) Plot of saturation island density as a function of the deposition rate F on surface at 200 K, yielding a scaling exponent χ equal to 0.26 ± 0.03 .

the deposition rate F on the Au(100) surface. The rate F has been calibrated by determining the Rutherford backscattering of gold deposited on silicon. By varying the flux by a factor of ~ 50 , we have, as illustrated in Fig. 6, found that $\chi = 0.26 \pm 0.03$. The value of the exponent χ is that expected for highly anisotropic (one-dimensional) diffusion and a critical cluster size of unity, as assumed in our analysis.

That diffusion is unidirectional seems to be confirmed by Fig. 7, which was taken at $T = 100$ K under manipulation conditions, after neon sputtering at ~ 150 eV for 20 min. After sputtering, gold atoms are present on the surface. Scanning the surface horizontally, starting at the bottom of the image, reveals the path of a single adatom propelled over the surface by the tip. The adatom moves over a considerable distance along one $\langle 01\bar{1} \rangle$ atom row until, as indicated by arrows, it jumps to an adjacent one, where it continues its motion, which demonstrates that diffusion in the $\langle 011 \rangle$ direction is preferred. This strong preference in the direction indicates an easy path for adatom diffusion. We believe that this preference is caused by the structure of the surface. In a subsequent image the adatom does not appear, most likely having become attached to the scanning tip and being removed.

III. DISCUSSION

Our result of 0.32 eV for the activation energy of self-diffusion is in good agreement with the value of 0.35 eV reported by Liu *et al.*¹⁴ on the presumption of two-dimensional motion and a critical island size equal to one. Our value for the activation energy was, however, derived for anisotropic motion, as was the barrier of ~ 0.2 eV of Günther *et al.*¹¹ obtained at a much higher temperature $T \geq 315$ K. Under these conditions it is likely that gold dimers will be mobile and may influence the saturation island density. At the much lower temperatures explored by us, only single atoms are likely to diffuse.

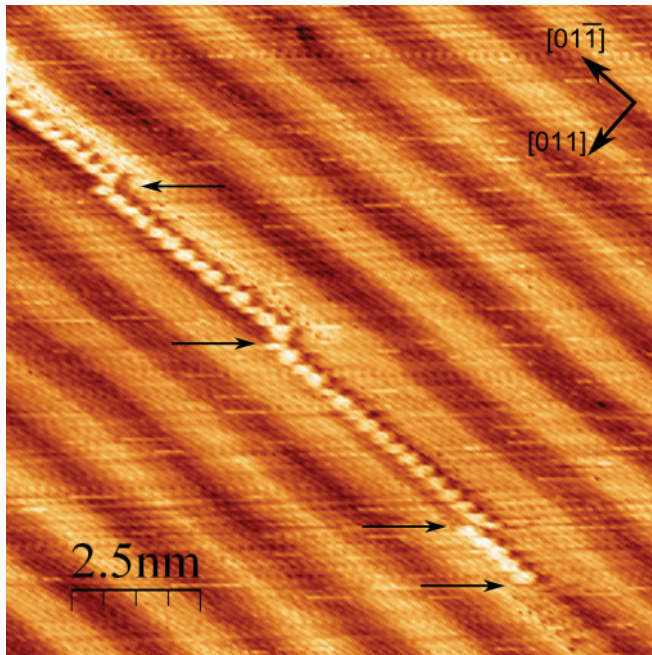


FIG. 7. (Color online) STM image of a gold adatom, produced by neon sputtering, moved over the reconstructed Au(100) by the scanning tip. Scanning at 100 K under manipulation conditions, at 20 nA and 12 mV, is along the horizontal, from the bottom to the top. The adatom moves over an appreciable length along one $[0\bar{1}1]$ atom row, until as indicated by arrows, it jumps to an adjacent one, where it continues its movement. A subsequent STM image does not show the atom.

Because we know the deposition rate to be 0.0025 ML/min (with 1 ML = 1×10^{15} atoms/cm²) and the coverage θ is 0.18, we find from the intercept of the diffusivity at infinite temperature, a frequency prefactor of $2(\times 4^{\pm 1}) \times 10^{13}$ s⁻¹. We can now also raise the obvious question—why did we only analyze the curve of the island density above 156 K? The answer is that the ratio of D/F amounts to 5×10^6 at $T = 150$ K but is only 3×10^4 at 125 K, below the limit of 10^5 for obtaining a reasonable diffusivity; at these low temperatures the island density is no longer adequately given by simple nucleation theory,¹² so these measurements have to be disregarded.

A surface structure similar to that of hex-Au(100) is that of hex-Pt(100),¹⁶ and Linderoth *et al.*¹⁷ have used an STM to examine the self-diffusion of platinum on this surface. For anisotropic diffusion and a critical island size of one, they arrived at an activation energy of 0.43 eV for surface diffusion. The ratio of the activation energy to the heat of sublimation is 0.0814, compared to 0.0943 for our results for hex-Au(100), a ratio typical for surface self-diffusion on similarly structured surfaces.¹⁸ In contrast, the diffusion energy of Günther *et al.*,¹¹ ~ 0.2 eV, gives a much lower ratio of only 0.058, which does not correspond with the value for hex-Pt(100).

For nonreconstructed Pt(100), diffusion has been observed to occur by exchange with the substrate,¹⁹ which is also the mechanism indicated in several theoretical studies^{20–29} for both Pt(100) and Au(100). It is, however, not clear that on the reconstructed surface exchange is a significant mechanism. It may well be that the compression of the reconstructed surface is able to eliminate the exchange mechanism from the picture.²⁸ For hex-Au(100) as well as hex-Pt(100), there are no experimental indications available for the mechanism of diffusion, and we must emphasize that there is no information about the diffusion mechanism emerging from our studies.

IV. CONCLUSIONS

We have demonstrated that diffusion of gold over the hex-reconstructed Au(100) surface is one dimensional and proceeds primarily along the $\langle 011 \rangle$ channels created during reconstruction. The exchange process suggested for unreconstructed Au(100) is most likely suppressed by the compression of the surface layer, but no direct information is available about the diffusion mechanism on the reconstructed Au(100) surface. However, we have identified an effective barrier of 0.32 ± 0.02 eV and a frequency prefactor of $2(\times 4^{\pm 1}) \times 10^{13}$ s⁻¹ to unidirectional surface self-diffusion.

ACKNOWLEDGMENTS

This work was carried out with support under AFOSR Grant No. AF FA9550-09-1-0248. We also appreciate the assistance of Tomasz Olewicz with the diagrams and of Vania Petrova with the experiments.

*Corresponding author: atrembulowicz@ifd.uni.wroc.pl

¹D. G. Fedak and N. A. Gjostein, *Surf. Sci.* **8**, 77 (1967).

²M. A. van Hove, R. J. Koestner, P. C. Stair, J. P. Biberian, L. Kesmodel, I. Bartos, and G. A. Somorjai, *Surf. Sci.* **103**, 189 (1981).

³M. A. van Hove, J. Koestner, P. C. Stair, J. P. Biberian, L. Kesmodel, I. Bartos, and G. A. Somorjai, *Surf. Sci.* **103**, 218 (1981).

⁴K. H. Rieder, T. Engel, R. H. Swedsen, and M. Manninen, *Surf. Sci.* **127**, 223 (1983).

⁵O. K. Binnig, H. Rohrer, C. Gerber, and E. Stoll, *Surf. Sci.* **144**, 321 (1984).

⁶K. Yamazaki, K. Takayanagi, Y. Tanishiro, and K. Yagi, *Surf. Sci.* **199**, 595 (1988).

⁷S. G. J. Mochrie, D. M. Zehner, B. M. Ocko, and D. Gibbs, *Phys. Rev. Lett.* **64**, 2925 (1990).

⁸D. Gibbs, B. M. Ocko, D. M. Zehner, and S. G. J. Mochrie, *Phys. Rev. B* **42**, 7330 (1990).

⁹B. M. Ocko, D. Gibbs, K. G. Huang, D. M. Zehner, and S. G. J. Mochrie, *Phys. Rev. B* **44**, 6429 (1991).

¹⁰P. Havu, V. Blum, V. Havu, P. Rinke, and M. Scheffler, *Phys. Rev. B* **82**, 161418(R) (2010)

¹¹S. Günther, E. Kopatzki, M. C. Bartelt, J. W. Evans, and R. J. Behm, *Phys. Rev. Lett.* **73**, 553 (1994).

¹²H. Brune, *Surf. Sci. Rep.* **31**, 121 (1998).

¹³J. W. Evans and M. C. Bartelt, *J. Vac. Sci. Technol. A* **12**, 1800 (1994).

¹⁴S. Liu, L. Bönig, and H. Metiu, *Phys. Rev. B* **52**, 2907 (1995).

- ¹⁵M. C. Bartelt, S. Günther, E. Kopatzki, R. J. Behm, and J. W. Evans, *Phys. Rev. B* **53**, 4099 (1996).
- ¹⁶G. Ritz, M. Schmid, P. Varga, A. Borg, and M. Ronning, *Phys. Rev. B* **56**, 10518 (1997).
- ¹⁷T. R. Linderoth, J. J. Mortensen, K. W. Jacobsen, E. Laegsgaard, I. Stensgaard, and F. Besenbacher, *Phys. Rev. Lett.* **77**, 87 (1996).
- ¹⁸G. Antczak and G. Ehrlich, *Surface Diffusion: Metals, Metal Atoms, and Clusters* (Cambridge University Press, Cambridge, 2010), p. 404.
- ¹⁹G. L. Kellogg and P. J. Feibelman, *Phys. Rev. Lett.* **64**, 3143 (1990).
- ²⁰C. L. Liu, J. M. Cohen, J. B. Adams, and A. F. Voter, *Surf. Sci.* **253**, 334 (1991).
- ²¹P. J. Feibelman and R. Stumpf, *Phys. Rev. B* **59**, 5892 (1999).
- ²²J. Zhuang and L. Liu, *Phys. Rev. B* **59**, 13278 (1999).
- ²³W. Xiao, P. A. Greaney, and D. C. Chrzan, *Phys. Rev. B* **70**, 033402 (2004).
- ²⁴C. M. Chang and C. M. Wei, *Chin. J. Phys.* **43**, 169 (2005).
- ²⁵S. Y. Kim, I.-H. Lee, and S. Jun, *Phys. Rev. B* **76**, 245407 (2007).
- ²⁶G. Boisvert, L. J. Lewis, and A. Yelon, *Phys. Rev. Lett.* **75**, 469 (1995).
- ²⁷G. Boisvert and L. J. Lewis, *Phys. Rev. B* **54**, 2880 (1996).
- ²⁸B. D. Yu and M. Scheffler, *Phys. Rev. B* **56**, R15569 (1997).
- ²⁹J. E. Müller and H. Ibach, *Phys. Rev. B* **74**, 085408 (2006).